





# Geophysical Research Letters<sup>®</sup>

## RESEARCH LETTER

10.1029/2022GL101856

## The 2013 Slab-Wide Kamchatka Earthquake Sequence

B. Rousset<sup>1</sup> , M. Campillo<sup>2</sup>, N. M. Shapiro<sup>2</sup> , A. Walpersdorf<sup>2</sup> , N. Titkov<sup>3</sup> , and D. V. Chebrov<sup>3,4</sup>

### Key Points:

- The  $M = 8.3$  Okhotsk deep-focus earthquake has been preceded by four intense shallow seismic clusters
- GNSS times series analysis reveals a transient event in April 2013 coincident in time with a doubling of intermediate-depth seismicity rate
- The ensemble of observations suggest a transient acceleration of the slab plunge in the months before the  $M = 8.3$  mainshock

### Supporting Information:

Supporting Information may be found in the online version of this article.

### Correspondence to:

B. Rousset,  
baptiste.rousset@unistra.fr

### Citation:

Rousset, B., Campillo, M., Shapiro, N. M., Walpersdorf, A., Titkov, N., & Chebrov, D. V. (2023). The 2013 slab-wide Kamchatka earthquake sequence. *Geophysical Research Letters*, 50, e2022GL101856. <https://doi.org/10.1029/2022GL101856>

Received 25 OCT 2022

Accepted 22 DEC 2022

### Author Contributions:

**Conceptualization:** B. Rousset, M. Campillo, N. M. Shapiro  
**Data curation:** A. Walpersdorf, N. Titkov, D. V. Chebrov  
**Formal analysis:** B. Rousset  
**Funding acquisition:** M. Campillo, N. M. Shapiro  
**Methodology:** B. Rousset, M. Campillo, N. M. Shapiro  
**Project Administration:** M. Campillo, N. M. Shapiro  
**Software:** B. Rousset  
**Writing – original draft:** B. Rousset

© 2023. The Authors.

This is an open access article under the terms of the [Creative Commons Attribution-NonCommercial-NoDerivs License](https://creativecommons.org/licenses/by-nc-nd/4.0/), which permits use and distribution in any medium, provided the original work is properly cited, the use is non-commercial and no modifications or adaptations are made.

<sup>1</sup>Institut Terre et Environnement de Strasbourg, UMR7063, Université de Strasbourg/EOST, CNRS, Strasbourg, France, <sup>2</sup>Institut des Sciences de la Terre, Université Grenoble Alpes, CNRS, Grenoble, France, <sup>3</sup>Schmidt Institute of the Physics of the Earth, Russian Academy of Sciences, Moscow, Russia, <sup>4</sup>Kamchatka Branch of the Geophysical Service, Russian Academy of Sciences, Petropavlovsk-Kamchatsky, Russia

**Abstract** Studies of initiation of large earthquakes are usually focused on frictional instabilities occurring in the near vicinity of the future rupture. Possible contributions of long-distance interactions with large-scale tectonic instabilities remain unknown. Here we analyze seismic catalogs and geodetic time series during a few months preceding the 2013  $M = 8.3$  deep-focus Okhotsk earthquake. This deep-focus event is preceded by four intense seismic clusters in the seismogenic zone. GNSS time series in Kamchatka revealed a transient landward motion episode 1 month prior to the mainshock, consistent with an increase of seismogenic zone loading. This transient loading episode is accompanied by a doubling of the intermediate depth seismicity rate suggesting a transient slab pull as the origin. These observations question the constant subducting velocity hypotheses and may have implications in the understanding of the long-distance along-slab stress interactions and in their contribution to initiation of large deep-focus earthquakes.

**Plain Language Summary** Subduction zone earthquakes are illuminating the dynamics of oceanic plates plunging into the mantle. In this study we analyzed the earthquake activity in the Kamchatka subduction zone before a 620 km deep  $M = 8.3$  earthquake that happened in 2013. This so-far largest recorded deep event was preceded by a large number of smaller seisms happening at much shallower depths, between the trench and 100 km depth. The analysis of surface deformation during this episode shows an increased horizontal compression of the Kamchatka peninsula. These observations and associated models together suggest an acceleration of the subduction plunging, interpreted as a mechanical link between the shallow intense seismicity and the large deep event.

## 1. Introduction

The subducting velocity of oceanic plates below the continental crust is primarily set by a force balance resulting from two processes: the adjunction of new oceanic crust at oceanic ridges associated with mantle convection that pushes the oceanic plate away: the ridge push, and the plunging into the mantle of the thickened and dense oceanic lithosphere: the slab pull. Depending on the age of the subduction zone, these two forces have different influences on the motion of the down-going plate (Schellart, 2004) and more specific parameters such as the bending of the oceanic lithosphere, lateral variations of viscosity and moving trenches can affect the subducting velocity (Becker & Faccenna, 2009; Lallemand et al., 2005).

In the infancy of plate tectonic theory, debates were active to understand whether plate motions are constant throughout the seismic cycles and in particular around times of large earthquakes (Anderson, 1975). With the improvement of space geodetic techniques in the 1980s, the decadal motions of the plates have been measured with centimetric precision. Comparisons between geological plate motions with magnetic anomalies and decadal geodetic measurements have shown that the inner oceanic plates are moving on average steadily at time scales of 3 Ma (DeMets et al., 1990; Gordon, 1991). The constant plate motions are now commonly extended to constant subducting velocities in most geodynamic and seismic cycle models at time scales of days to years. Measurable perturbations relative to the average steady motion are thought to arise from frictional instabilities in the vicinity of the seismogenic zone of plate boundaries such as regular earthquakes or recently discovered slow slip events (Dragert et al., 2001). Similarly, the possible preparation phase leading to the generation of large earthquakes is mainly considered in the framework of the near-rupture processes (Kato & Ben-Zion, 2021). However, possible larger scale subducting velocity perturbations have been hypothesized with observations of a synchronization between the deep seismicity and the large shallow earthquakes (Mogi, 1973, 2004), suggested to mark the acceleration of the slab plunge that contributes to the nucleation of the latter (Bouchon et al., 2016).

Writing – review & editing: B. Rousset, M. Campillo, N. M. Shapiro, A. Walpersdorf, N. Titkov, D. V. Chebrov

In this article, we report a detailed analysis of seismicity and ground displacement during the months preceding the  $M = 8.3$  Okhotsk sea earthquake that occurred on 24 May 2013. The observations have been recorded by a regional seismic network (Chebrov et al., 2013; Chebrova et al., 2020) and continuous GNSS stations operated by the Kamchatka Branch of the Geophysical Survey of the Russian Academy of Science (KBGS RAS) (Shestakov et al., 2014). This deep-focus event originated in the Kamchatka subduction zone that accommodates 80 mm/yr of motion between the Pacific plate and the Okhotsk plate, a microplate part of the larger North America plate (Seno et al., 1996). The subduction terminates at  $56^\circ\text{N}$ , where the trench intersects the Aleutian arc (Levin et al., 2002, 2005). The slab interface has a dip angle of  $55^\circ$  south of  $55^\circ\text{N}$  down to depths of 600 km. North of  $55^\circ\text{N}$ , the broken slab stops at 300 km depth and the dip angle diminishes to  $35^\circ$  (Gorbatov et al., 1997; I. Y. Koulakov et al., 2011). The seismogenic section of the subduction has ruptured in five historical large earthquakes of  $M > 8.0$  in the 20th century, the largest being a  $M = 9.0$  earthquake in 1952 (Johnson & Satake, 1999; MacInnes et al., 2010). Geodetic measurements show a high interseismic locking of the seismogenic zone where the locked areas coincide spatially with historical earthquake asperities (Bürgmann et al., 2005).

The 2013 deep-focus  $M = 8.3$  earthquake occurred at  $\sim 620$  km depth and produced horizontal and vertical surface displacements of up to 15 mm, recorded both by regional seismic and geodetic networks. The surface deformation can be modeled with a dislocation on a low eastward dipping plane compatible with the double couple focal mechanism, with slip amplitudes of a few meters (Shestakov et al., 2014; Steblou et al., 2014). The stress drop is 12–15 MPa, which is similar to the stress drops of shallow megathrust earthquakes, and an order of magnitude lower than the other historical deep-focus earthquake of  $M > 8$  that happened in Bolivia in 2015 (Ye et al., 2013; Zhan et al., 2014). The mainshock has been followed by few aftershocks, which is common for large deep earthquakes. A  $M = 6.7$  event is noticeable a few hours after and 200 km south of the mainshock, producing larger stress drops, possibly as a result of lateral stress heterogeneities within the slab.

## 2. Seismicity Observations

In this study, we use the earthquake catalog created with the routine analysis at the KBGS RAS. This analysis is based on records of the Kamchatka regional network (Chebrov et al., 2013). Both the network configuration and the earthquake determination approach (Droznin & Droznina, 2011) have not been significantly modified since 2011. KBGS RAS uses the modified regional magnitude scale (Gusev & Melnikova, 1990). The completeness magnitude over the Kamchatka - northern Kuril Islands regions is estimated to be  $M_l = 3.5$  (Chebrov et al., 2013; Levina et al., 2013) and even lower in some areas (Saltykov, 2019). Therefore, we only analyze earthquakes with  $M_l \geq 3.5$  which is still much lower than available from global catalogs. Most of the stations of the network are installed in the Kamchatka peninsula and are located west of the Kuril-Kamchatka trench. With such one-sided station coverage, the hypocenter locations for earthquakes in the shallow part of the Benioff zone are subject to significant trade-offs between the lateral position and the depth with the errors in the letter reaching a few tens of kilometers (Droznin et al., 2019). KBGS RAS does not provide earthquake focal mechanisms in their catalog. Therefore, in our analysis we use Global Centroid Moment Tensor (GCMT) focal mechanisms (Ekström et al., 2012).

In this study, we focus on the months prior to the 2013 deep-focus  $M = 8.3$  mainshock. During these months, the seismicity at large depths was very quiet. Two noticeable events of  $M = 7.7$  at  $\sim 630$  km depth and  $M = 7.3$  at  $\sim 500$  km depth happened in July and November of 2008, 5 years before. While seismicity was quiescent at large depths, an exceptionally intense seismic activity happened at shallow depths (Figures 1 and 2). Within the

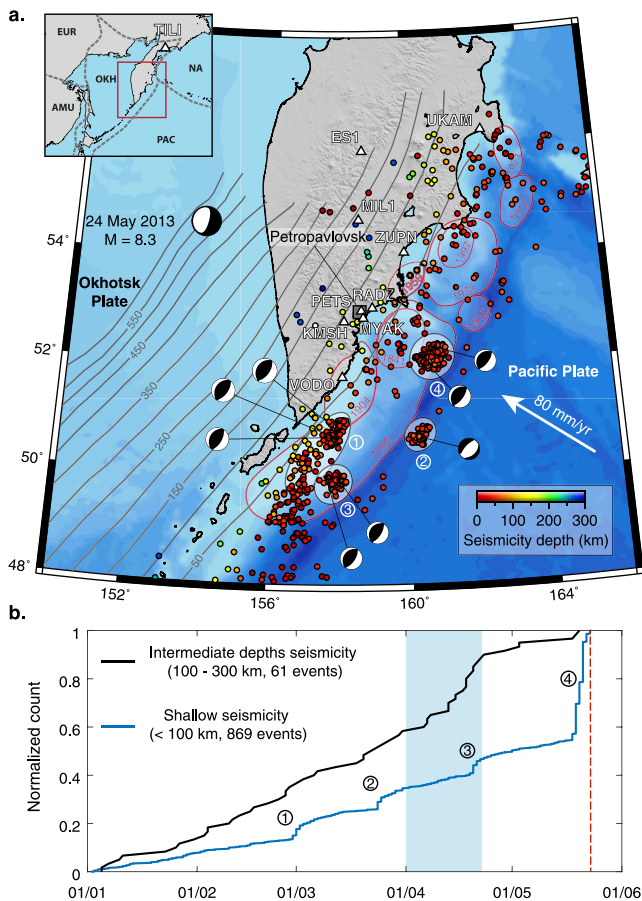


**Figure 1.** Tectonic context and early 2013 earthquakes. (a) Along the Kamchatka trench, the Pacific plate subducts below the Okhotsk plate at a rate of 8 cm/yr. In the months before the deep-focus  $M = 8.3$  earthquake, the shallow seismicity is organized in spatial clusters, color-coded by their depth. The GCMT seismic moment tensors (Ekström et al., 2012) are represented for events of  $M_l > 6$ . The red contours indicate the rupture areas of large historic earthquakes determined from aftershock distributions (Johnson & Satake, 1999) also represented in Bürgmann et al. (2005). The gray lines indicate the slab contours (Hayes et al., 2018). The white triangles show the locations of GNSS sites. The inset indicates the surrounding tectonic plates. PAC: Pacific; NA: North America; EUR: Eurasia; OKH: Okhotsk; AMU: Amuria. (b) Normalized count of earthquakes for depths  $< 100$  km and between 100 and 300 km. The numbers denote the shallow clusters also presented on the map. The red dashed line indicates the timing of the  $M = 8.3$  deep-focus event. The light blue rectangle shows the timing of the transient event observed in the GNSS time series.

three first months of 2013, four clusters at depths shallower than 100 km released an important accumulated moment (cluster 1: 75 events,  $M_0 = 4.9 \times 10^{19}$  N·m; cluster 2: 56 events,  $M_0 = 4.0 \times 10^{18}$  N·m; cluster 3: 75 events,  $M_0 = 1.6 \times 10^{19}$  N·m; cluster 4: 399 events,  $M_0 = 2.4 \times 10^{19}$  N·m, Figure 1). Half of the  $M_l > 6$  events from 2010 to 2018 (13 over 26) happened during these seismic clusters (Figure 2). The four clusters are all located at the edges of the historical rupture area of the historical  $M = 9.0$  earthquake of 1952 (Johnson & Satake, 1999; MacInnes et al., 2010) (Figure 1). The GCMT seismic moment tensors (Ekström et al., 2012) for  $M_l > 6$  events show reverse focal mechanisms for the clusters 1, 3, and 4 and a normal focal mechanism associated with the outer-rise events of the cluster 2. The last cluster with  $\sim 6$  times more events than the three other clusters, spanning depths from 0 to 100 km, occurred from 19 May to 22 May, two days before the deep-focus mainshock. In the GCMT catalog, 28 similar reverse focal mechanisms are computed for events with  $M_l$  between 4.8 and 6.1 during the fourth cluster. Looking at the  $M_l$  of individual events within the clusters (Figure S2 in Supporting Information S1), the outer-rise cluster 2 seems dominated by a mainshock aftershock sequence. Clusters 1 and 3 still have events of large  $M_l$  after the mainshocks, suggesting a mix of mainshock aftershock sequences together with swarms. The cluster 4 is however clearly a large swarm, without event of dominant  $M_l$ . At intermediate depths, between 100 and 300 km, a steady seismicity rate is observed during these months with a transient doubling of the rate early April 2013, during  $\sim 18$  days ( $M_0 = 1.3 \times 10^{16}$  N·m). During this transient seismicity increase, events were not spatially clustered like in the shallow seismic clusters, but were spread over a large area (Figure S1 in Supporting Information S1). This intense seismic activity at intermediate depths is unusual when looking at a 10-year long catalog of seismicity. Other than in April 2013, such seismicity rates only happened during aftershock sequences following large earthquakes in 2013 and 2016 (Figure 2 and Figure S3 in Supporting Information S1).

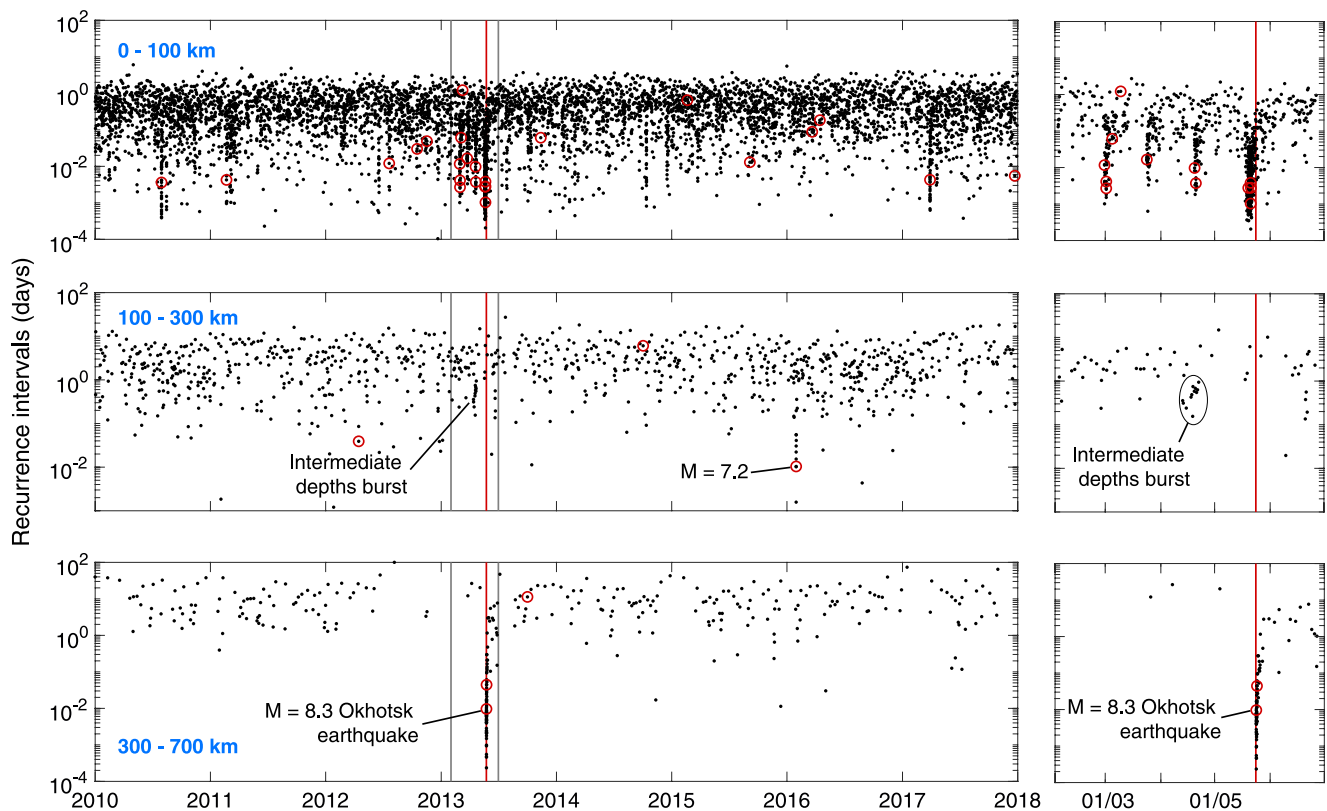


**Figure 2.** Seismicity activity as a function of depth. The duration since previous earthquakes in logarithmic scale is represented as a function of time from 2010 to 2018 in the left panels. The depth bins are specified in blue. The right panels show a zoom on the period 01 February 2013 to 01 July 2013, delimited with the gray lines on the left panels. The red circles indicate events with  $M_l > 6.0$ . The time of the  $M = 8.3$  Okhotsk earthquake is shown by the red line.

### 3. GNSS Observations

The GNSS data used in this study have been recorded by 10 continuous stations operated and maintained by the KBGS RAS. We have processed the time series for a 10-year period of time, from 2005 to 2015. Most of the sites have been active only a few years over the 10 years. Detailed GNSS analysis is described in Supporting Information S1. At first look, the 10-year long time series show transient oscillating signals with annual periods that are mainly seen by the vertical components but also on horizontal components.

When scrutinizing the months in early 2013, we could not detect any signal associated with the shallow seismic clusters. However, we identified a transient event early April 2013, with a duration estimated to be between 16 and 22 days depending on the GNSS sites, with average duration of 18 days, that coincides in time with the transient increase of intermediate depth seismicity rates (Figure S4 in Supporting Information S1). This transient is mainly captured on the east position components. Transient signals in GNSS time series with duration of a few weeks can have various sources. They can either be common mode errors due to propagation of orbital or reference frame errors. Common mode errors have the same amplitude on all sites of a local network. The second possible source is related to surface water loading due to precipitations of rain or snow, with a dominant annual period and usually important local variations from site to site. The third possible source is tectonic and produces specific deformation patterns at the surface which depend on the physical processes at depth. We compared the transient event observed in 2013 with all other years available (Figure 3). This event seems unusual compared to all other years, and the deviation in 2013 from other years is more significant at sites close to the coast (e.g., PETS, RADZ). Also, the spatial pattern of the transient signal (Figure 4a) is specific, with larger amplitudes at the eastern coast (e.g., VODO, RADZ) then inland (e.g., ES1). This pattern is very similar to the decadal-estimated interseismic velocity field (Figure S7 in Supporting Information S1). The transient is not recorded at sites far from the subduction like TILI located at 62°N (Figure 1), thus discarding the common mode hypothesis. We also looked at independent observations to evaluate the surface loading hypothesis. The transient snow melt episode recorded with satellite images show that the melting occurred from mid-May to mid-June (Figure S5 in Supporting Information S1), more than a month after the observed GNSS transient. Given the larger amplitude at coastal sites, a possible ocean loading episode should be considered. We looked at the surface sea height anomalies along the Kamchatka coastline recorded with altimetry satellites (Figure S6 in Supporting Information S1), and no unusual transient ocean loading event is recorded in April 2013.

The surface pattern of the transient event being similar to the interseismic loading pattern (Figure S7 in Supporting Information S1) and the concomitance with the acceleration of intermediate depth seismicity rates (Figure S4

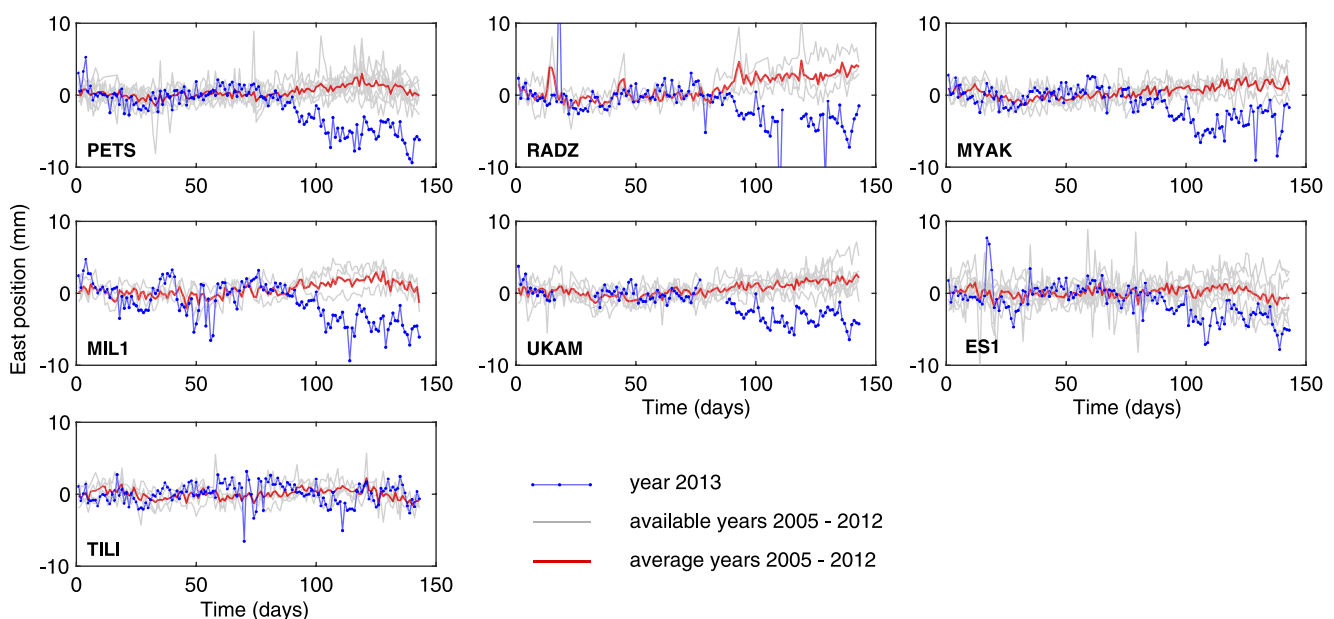


**Figure 3.** GNSS time series early 2013 compared to other years. The blue lines correspond to the GNSS times series during the first 143 days of 2013, the gray ones to all the available time series between 2005 and 2012 and the red time series is the average of all the gray ones.



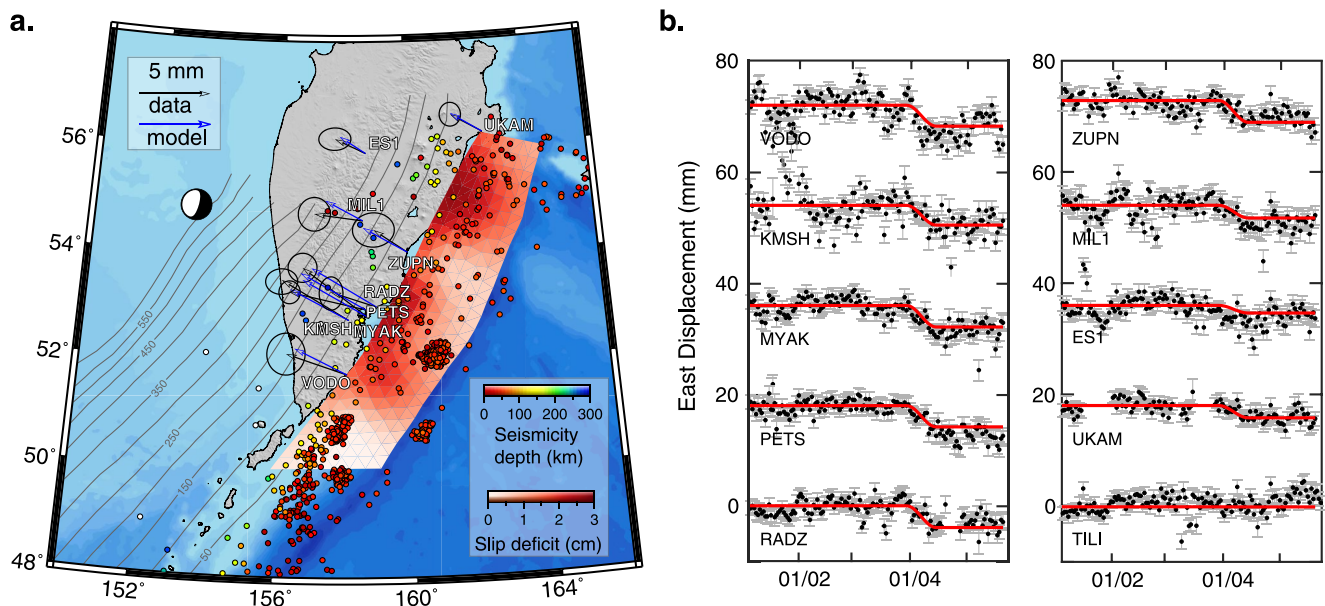


**Figure 4.** Seismogenic zone slip deficit inverse model of the transient loading event. (a) Map showing the static offsets of the transient loading event in black and the model predictions in blue. Slip deficit with amplitudes between 0 and 3 cm during a period of 18 days is shown with the red color-scale. Earthquakes that happened in 2013 before the Okhotsk earthquake are also shown, color-scaled by depth. (b) East GNSS position time series in black and model prediction time series in red.

in Supporting Information S1) both suggest that a tectonic origin associated with the subduction zone is the most likely. Compared to the well-known transient slow slip events that are releasing part of the accumulated stress below the seismogenic zone at some subduction zones (Dragert et al., 2001), the displacements of the April 2013 transient deformation event are not trenchward, but landward. Figure S6 in Supporting Information S1 compares the interseismic velocities relative to fixed Eurasian plate and computed over a period of 8 years (Figure S7 in Supporting Information S1) with the velocities during the transient event. The directions of the two velocity fields are very compatible, but the amplitudes of the velocities during the transient event are about 3.2 times larger than the ones during the interseismic period (Figure S7b in Supporting Information S1), suggesting a transient increased loading event.

#### 4. Kinematic Modeling

In order to obtain a tectonic explanation to the transient deformation observed with GNSS observations in April 2013, we consider dislocations compatible with the subduction interface model slab 2.0 (Hayes et al., 2018) at a range of depths from the trench to the bottom of the slab at 600 km depth as well as on the coseismic rupture plane published by Ye et al. (2013). For each model considered, we computed slip and slip deficit. The detailed modeling strategy is described in Supporting Information S1. The RMS error for both slip and slip deficit models are given in Table S1 in Supporting Information S1. To explain the landward motion of the transient event, all models located between the trench and 400 km depth have lower RMS errors with slip deficit, which suggest an increase of loading of the upper plate. Best models at deeper depths are compatible with actual slip, suggesting a release of accumulated stress. When comparing these different depth models (Figures S8 and S9 in Supporting Information S1), in which the rake angle is fixed in the direction of the convergence, only the ones at seismogenic depths are able to fit the transient deformation polarities at all the stations of the GNSS network. Other models, and in particular the deepest ones, are not able to explain the northern sites polarities. One reason is the deep slab break-off for latitude higher than 55°N. The RMS error for the slip deficit model in the seismogenic zone is more than two times lower than the RMS errors of all the deeper models tested. We thus conclude that the surface transient deformation event is likely due to slip deficit on the seismogenic zone at depths lower than 60 km. Without the slab break-off north of 55°N, the signal could have been explained by a deep slip episode. Although the seismogenic zone slip deficit model is the most simple to explain the data, it is possible that deeper transient slip participates in the observed surface deformation.

The best forward model with homogeneous slip deficit on the seismogenic zone has a root mean square (RMS) error of 0.93 mm for a slip deficit amplitude of 1.4 cm (Figures S8a and S8c in Supporting Information S1). The preferred inverse slip deficit model with a correlation length  $\lambda = 300$  km has a RMS error of 0.78 mm. The fit to the east position time series with largest signal amplitudes is presented in Figure 4 and the fit to the north position time series is presented in Figure S10 in Supporting Information S1. The gain of RMS error between the inverse model with lateral slip deficit variations and the forward model with homogeneous slip deficit is 15%. This small gain shows that the main parameter explained by the GNSS transient offsets is the amplitude of the transient slip deficit, rather than the roughness of the lateral variations.

The interseismic locking  $C$  defined as the ratio between slip deficit rate  $\delta$  and a reference velocity  $V_r$ :  $C = \frac{\delta}{V_r}$  is a classical metric to define the degree of locking of the seismogenic zone (e.g., Avouac, 2015). The reference velocity  $V_r$  corresponds to the interseismic subducting velocity of the subduction below the seismogenic zone. The long-term convergence velocity estimated at the trench is often considered as the reference velocity. In order to estimate the locking of the seismogenic zone during the 2013 transient event in Kamchatka, we consider an average slip deficit of 1.4 cm over a duration of 18 days. If we assume the long-term steady-state convergence velocity at the trench of 80 mm/yr, we obtain an average value of locking  $C = 3.6$ , which is physically impossible. Because the locking cannot be larger than 1, the reference velocity during this transient episode cannot be considered as the long-term convergence velocity at the trench. Assuming that the seismogenic zone locking keeps high values close to one as it was in average during the previous decades (Bürgmann et al., 2005), the reference velocity has to be  $\sim 3.6$  higher than the long-term convergence velocity to reach amplitudes of  $\sim 28.8$  cm/yr. Given that the slip deficit amplitude of 1.4 cm during the transient deformation episode corresponds to an upper bound since part of the signal could also be explained by deeper transient slip, the increase of the reference velocity by 3.6 also corresponds to an upper limit of acceleration. Since the subducting velocity at the seismogenic zone results from a force balance between the ridge push and the slab pull, one of these two forces has to transiently increase. No evidence tend to show an increase of the ridge push, however, the simultaneous increase of intermediate depth seismicity rate together with the subsequent deep-focus  $M = 8.3$  event suggest an increased transient deformation at depth related to a transient slab pull acceleration.

## 5. Discussion

In the months before the  $M = 8.3$  deep-focus Okhotsk earthquake, four intense seismic clusters happened in the seismogenic zone and outer-trench, 500–600 km above the large mainshock. The analysis of GNSS time series shows a transient signal which is best explained with a transient slip deficit on the seismogenic zone, compatible with a transient loading of the forearc. This transient event coincides in time with a doubling of intermediate depth earthquakes rate. Figure 5 shows an interpretation of the sequence of events that could explain the ensemble of observations. At steady-state, the subducting velocity is set by a balance between the ridge push and the slab pull forces that are both steady. The slab pull force results from the weight of the slab that pulls it inside the mantle and the viscous drag of the overriding mantle that resists the down-going motion. At shallow depths, the locked seismogenic zone compresses the forearc and produces landward motion of the GNSS often referred to as interseismic motion (Bürgmann et al., 2005). A disturbance from this steady-state system might be coming from a transient reduced viscous drag. Numerical simulations including a low viscosity zone on the subduction interface show that it could significantly increase the subducting velocity (Behr et al., 2022). The transient decrease of apparent viscosity of the slab interface could be due to increased fluid flow along the plate interface, knowing that slabs are thought to transport significant amounts of water to the deep mantle (Ohtani, 2005). Another possible explanation is partial melting at intermediate depths below the active volcanic arc, reducing the viscosity at the slab interface shear zone (Behr et al., 2021). The Kamchatka volcanic arc is one of the most active on earth with large melt volume production. Also, because of the proximity to the northern termination of the subduction, the toroidal mantle flow around the edge of the plate (Levin et al., 2005; Yogodzinski et al., 2001; Peyton et al., 2001; I. Koulakov et al., 2020; Zhao et al., 2021) might modify melting conditions of the oceanic plate and have an influence on the subduction dynamics.

The transient reduced drag of the down-going plate induces a slab plunge acceleration that produces extension at intermediate and shallow depths resulting in increased intermediate depths seismicity rates and might also compress the bottom of the inner-slab. The increase of the slab pull force modifies the subducting velocity below the seismogenic zone. Given that the seismogenic zone is locked, the compression of the forearc is also increasing,

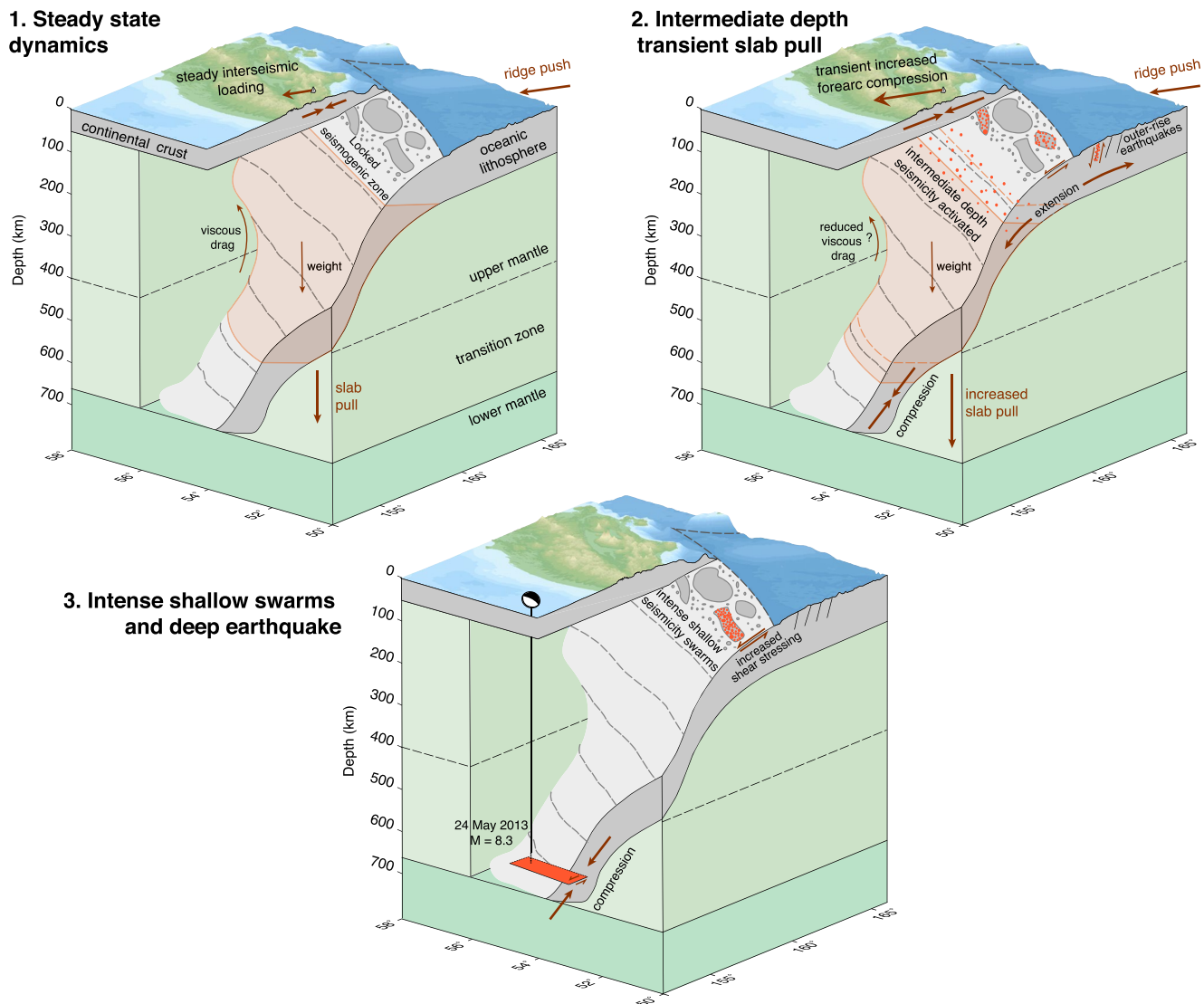


**Figure 5.** Interpretational sketch for the 2013 Kamchatka sequence. (1) Steady-state phase during which the interseismic loading is constant, with constant ridge push and slab pull forces. The motion of the locked seismogenic zone compresses the forearc. The interseismic loading is observed by westward GNSS velocities. (2) Intermediate depth transient slab pull. The large-scale deformation of the slab induces an extension at intermediate depths that resulted in increased seismicity rates and a possible compression of the deep portion of the slab. This transient slab plunge increased the plate subducting velocity at the seismogenic zone that is translated in the GNSS time series as a transient increased loading event. (3) Shallow seismic clusters and large deep earthquake. The stress perturbations induced by the slab plunge induce large shallow seismic clusters both on the seismogenic zone and outer-trench and might have participated in the initiation of the  $M = 8.3$  deep Okhotsk earthquake.

as observed by the GNSS transient landward motion. We computed the coulomb stress change on the seismogenic zone associated with dip slip on the subduction interface below 60 km depth for an increased subducting velocity by 3.6 and it shows that the stress change on the seismogenic zone can get values up to 1 kPa. Such an amplitude is rather small, and likely cannot explain alone the triggering of the shallow swarms. This small amplitude, the time delay between the transient slab motion and the shallow seismic clusters and the swarm behavior of the seismic clusters indicate that the redistribution of stresses during this transient slab pull motion might have induced poroelastic fluid flow close to the seismogenic zone that triggered the intense swarm activity. Alternatively, the fact that shallow seismic swarms are happening before and after the transient deformation episode could also be due to a much longer duration of the transient slab pull, either continuous or as a cascade of several transient increased down-going motions, while only the fastest phase can be seen with GNSS observations.

On top of the intermediate depth extension, the transient slab pull could also have produced sub-vertical compression of the bottom inner-slab that might have played a role in the triggering of the deep-focus  $M = 8.3$  earthquake

that ruptured a near-horizontal eastward dipping plane (Ye et al., 2013) perpendicular to the compression a month later. Laboratory experiments show that acoustic emissions emerge for strain rates higher than 20% in the conditions of deep-focus earthquakes (Schubnel et al., 2013). The transient deep-slab compression might have participated to reach such a threshold.

Because GNSS and seismic signals are indirect consequences of the slab transient motion, we cannot quantify the exact volume displaced and the stresses induced at various depths of the subduction. Modeling of this large-scale subduction deformation event with realistic rheologies to reproduce an increase of subducting velocity at time scales of months could help quantifying these amplitudes. Such an event should have a viscoelastic response that might be measurable in GNSS time series in the following years. Modeling the viscoelastic response should help to constrain the associated transient rheologies. Finally, other observations, and in particular gravity measurements, might help obtaining constraints on the amplitude of the slab deformation (Bouh et al., 2022; Mikhailov et al., 2016; Panet et al., 2018).

This observation of a transient increase of the subducting velocity could have important implications for a better understanding of the deep-focus earthquake generation that might be the result of transient increased strain rate associated with slab plunge episodes. It also sheds light on slab-wide interactions between deep slab deformation and seismogenic zone activity. Finally, although this type of deviation from steady-state subducting motion might be rare, it potentially has implications for both large-scale geodynamic models and seismic cycle simulations in which the subducting velocities are often considered constant.

## Data Availability Statement

The data used in the work were obtained with large-scale research facilities “Seismic infrasound array for monitoring Arctic cryolitzone and continuous seismic monitoring of the Russian Federation, neighboring territories and the world.” The GNSS time series presented in this work can be found at: <https://doi.org/10.5281/zenodo.6817009>. The seismicity catalog used in our analysis is available from the website of the Kamchatkan Branch of Geophysical Survey of Russian Academy of Sciences: <http://sdis.emsd.ru/info/earthquakes/catalogue.php>.

## Acknowledgments

The authors thank Michel Bouchon for discussions about this study. B.R., M.C., and N.S. acknowledge support from the European Research Council (ERC) under the European Union's Horizon 2020 research and innovation program (Grant agreements no 742335, F-IMAGE for B.R. and M.C. and 787399, SEISMAZE for N.S.). N.S., D.C., and N.T. have been supported by Grant 14.W03.31.0033 of the Russian Ministry of Education and Science “Geophysical research, monitoring and forecasting of catastrophic geodynamic processes in the Russian Far East.”

## References

- Anderson, D. L. (1975). Accelerated plate tectonics. *Science*, 187(4181), 1077–1079. <https://doi.org/10.1126/science.187.4181.1077>
- Avouac, J.-P. (2015). From geodetic imaging of seismic and aseismic fault slip to dynamic modeling of the seismic cycle. *Annual Review of Earth and Planetary Sciences*, 43(1), 233–271. <https://doi.org/10.1146/annurev-earth-060614-105302>
- Becker, T. W., & Faccenna, C. (2009). A review of the role of subduction dynamics for regional and global plate motions. *Subduction zone geodynamics* (pp. 3–34). [https://doi.org/10.1007/978-3-540-87974-9\\_1](https://doi.org/10.1007/978-3-540-87974-9_1)
- Behr, W. M., Gerya, T. V., Cannizzaro, C., & Blass, R. (2021). Transient slow slip characteristics of frictional-viscous subduction megathrust shear zones. *AGU Advances*, 2(3), e2021AV000416. <https://doi.org/10.1029/2021AV000416>
- Behr, W. M., Holt, A. F., Becker, T. W., & Faccenna, C. (2022). The effects of plate interface rheology on subduction kinematics and dynamics. *Geophysical Journal International*, 230(2), 796–812. <https://doi.org/10.1093/gji/ggac075>
- Bouchon, M., Marsan, D., Durand, V., Campillo, M., Perfettini, H., Madariaga, R., & Gardonio, B. (2016). Potential slab deformation and plunge prior to the Tohoku, Iquique and Maule earthquakes. *Nature Geoscience*, 9(5), 380–383. <https://doi.org/10.1038/ngeo2701>
- Bouh, M., Panet, I., Remy, D., Longuevergne, L., & Bonvalot, S. (2022). Deep mass redistribution prior to the 2010 mw 8.8 Maule (Chile) earthquake revealed by grace satellite gravity. *Earth and Planetary Science Letters*, 584, 117465. <https://doi.org/10.1016/j.epsl.2022.117465>
- Bürgmann, R., Kogan, M. G., Steblov, G. M., Hilley, G., Levin, V. E., & Apel, E. (2005). Interseismic coupling and asperity distribution along the Kamchatka subduction zone. *Journal of Geophysical Research*, 110(B7), B07405. <https://doi.org/10.1029/2005JB003648>
- Chebrov, V., Droznin, D., Kugaenko, Y. A., Levina, V., Senyukov, S., Sergeev, V., et al. (2013). The system of detailed seismological observations in Kamchatka in 2011. *Journal of Volcanology and Seismology*, 7(1), 16–36. <https://doi.org/10.1134/S0742046313010028>
- Chebrova, A. Y., Chemarev, A., Matveenko, E., & Chebrov, D. (2020). Seismological data information system in Kamchatka branch of GS RAS: Organization principles, main elements and key functions. *Geophysical Research*, 21(3), 66–91. <https://doi.org/10.21455/gr2020.3-5>
- DeMets, C., Gordon, R. G., Argus, D., & Stein, S. (1990). Current plate motions. *Geophysical Journal International*, 101(2), 425–478. <https://doi.org/10.1111/j.1365-246X.1990.tb06579.x>
- Dragert, H., Wang, K., & James, T. S. (2001). A silent slip event on the deeper Cascadia subduction interface. *Science*, 292(5521), 1525–1528. <https://doi.org/10.1126/science.1060152>
- Droznin, D. V., & Droznina, S. Y. (2011). Interactive DIMAS program for processing seismic signals. *Seismic Instruments*, 47(3), 215–224. <https://doi.org/10.3103/S0747923911030054>
- Droznin, D. V., Droznina, S. Y., Senyukov, S. L., Chebrov, D. V., Shapiro, N. M., & Shebalin, P. N. (2019). Probabilistic estimates of hypocenters from the data of Kamchatka seismic network stations. *Izvestiya - Physics of the Solid Earth*, 55(4), 677–687. <https://doi.org/10.1134/S1069351319040049>
- Ekström, G., Nettles, M., & Dziewoński, A. (2012). The global CMT project 2004–2010: Centroid-moment tensors for 13,017 earthquakes. *Physics of the Earth and Planetary Interiors*, 200, 1–9. <https://doi.org/10.1016/j.pepi.2012.04.002>
- Gorbatov, A., Kostoglodov, V., Suárez, G., & Gordeev, E. (1997). Seismicity and structure of the Kamchatka subduction zone. *Journal of Geophysical Research*, 102(B8), 17883–17898. <https://doi.org/10.1029/96JB03491>



- Gordon, R. G. (1991). Plate motions are steady. *EOS, Transactions American Geophysical Union*, 72(10), 115. <https://doi.org/10.1029/eo0721010p00115-01>
- Gusev, A. A., & Melnikova, V. N. (1990). Correlations between world and Kamchatka magnitudes. *Journal of Volcanology and Seismology*, 6, 55–63.
- Hayes, G. P., Moore, G. L., Portner, D. E., Hearne, M., Flamme, H., Furtney, M., & Smoczyk, G. M. (2018). Slab2, a comprehensive subduction zone geometry model. *Science*, 362(6410), 58–61. <https://doi.org/10.1126/science.aat4723>
- Johnson, J. M., & Satake, K. (1999). Asperity distribution of the 1952 great Kamchatka earthquake and its relation to future earthquake potential in Kamchatka. *Pure and Applied Geophysics*, 541–553. [https://doi.org/10.1007/978-3-0348-8679-6\\_8](https://doi.org/10.1007/978-3-0348-8679-6_8)
- Kato, A., & Ben-Zion, Y. (2021). The generation of large earthquakes. *Nature Reviews Earth and Environment*, 2(1), 26–39. <https://doi.org/10.1038/s43017-020-00108-w>
- Koulakov, I., Shapiro, N. M., Sens-Schönfelder, C., Luehr, B. G., Gordeev, E. I., Jakovlev, A., et al. (2020). Mantle and crustal sources of magmatic activity of Klyuchevskoy and surrounding volcanoes in Kamchatka inferred from earthquake tomography. *Journal of Geophysical Research: Solid Earth*, 125(10), e2020JB020097. <https://doi.org/10.1029/2020JB020097>
- Koulakov, I. Y., Dobretsov, N., Bushenkova, N., & Yakovlev, A. (2011). Slab shape in subduction zones beneath the Kurile–Kamchatka and Aleutian arcs based on regional tomography results. *Russian Geology and Geophysics*, 52(6), 650–667. <https://doi.org/10.1016/j.rgg.2011.05.008>
- Lallemand, S., Heuret, A., & Boutelier, D. (2005). On the relationships between slab dip, back-arc stress, upper plate absolute motion, and crustal nature in subduction zones. *Geochemistry, Geophysics, Geosystems*, 6(9). <https://doi.org/10.1029/2005GC000917>
- Levin, V., Shapiro, N., Park, J., & Ritzwoller, M. (2002). Seismic evidence for catastrophic slab loss beneath Kamchatka. *Nature*, 418(6899), 763–767. <https://doi.org/10.1038/nature00973>
- Levin, V., Shapiro, N. M., Park, J., & Ritzwoller, M. H. (2005). Slab portal beneath the Western Aleutians. *Geology*, 33(4), 253–256. <https://doi.org/10.1130/G20863.1>
- Levina, V. I., Lander, A. V., Mityushkina, S. V., & Chebrova, A. Y. (2013). The seismicity of the Kamchatka region: 1962–2011. *Journal of Volcanology and Seismology*, 7(1), 37–57. <https://doi.org/10.1134/S0742046313010053>
- MacInnes, B. T., Weiss, R., Bourgeois, J., & Pinegina, T. K. (2010). Slip distribution of the 1952 Kamchatka great earthquake based on near-field tsunami deposits and historical records. *Bulletin of the Seismological Society of America*, 100(4), 1695–1709. <https://doi.org/10.1785/0120090376>
- Mikhailov, V. O., Diament, M., Lyubushin, A. A., Timoshkina, E. P., & Khairtadinov, S. A. (2016). Large-scale aseismic creep in the areas of the strong earthquakes revealed from the grace data on the time variations of the Earth's gravity field. *Izvestiya - Physics of the Solid Earth*, 52(5), 692–703. <https://doi.org/10.1134/S1069351316040054>
- Mogi, K. (1973). Relationship between shallow and deep seismicity in the Western Pacific region. *Tectonophysics*, 17(1), 1–22. [https://doi.org/10.1016/0040-1951\(73\)90062-0](https://doi.org/10.1016/0040-1951(73)90062-0)
- Mogi, K. (2004). Deep seismic activities preceding the three large ‘shallow’ earthquakes off south-east Hokkaido, Japan—The 2003 Tokachi-Oki earthquake, the 1993 Kushiro-Oki earthquake and the 1952 Tokachi-Oki earthquake. *Earth Planets and Space*, 56(3), 353–357. <https://doi.org/10.1186/BF03353064>
- Ohtani, E. (2005). Water in the mantle. *Elements*, 1(1), 25–30. <https://doi.org/10.2113/gselements.1.1.25>
- Panet, I., Bonvalot, S., Narteau, C., Remy, D., & Lemoine, J.-M. (2018). Migrating pattern of deformation prior to the Tohoku-Oki earthquake revealed by GRACE data. *Nature Geoscience*, 11(5), 367–373. <https://doi.org/10.1038/s41561-018-0099-3>
- Peyton, V., Levin, V., Park, J., Brandon, M., Lees, J., Gordeev, E., & Ozerov, A. (2001). Mantle flow at a slab edge: Seismic anisotropy in the Kamchatka region. *Geophysical Research Letters*, 28(2), 379–382. <https://doi.org/10.1029/2000GL012200>
- Saltykov, V. (2019). Possible problems of evaluation of spatial-temporal features of earthquake catalog representativity: Case study for the Kamchatka. *Catalog of Geophysical Survey of RAS*, 3(43), 66–74. <https://doi.org/10.31431/1816-5524-2019-3-43-66-74>
- Schellart, W. (2004). Quantifying the net slab pull force as a driving mechanism for plate tectonics. *Geophysical Research Letters*, 31(7). <https://doi.org/10.1029/2004GL019528>
- Schubnel, A., Brunet, F., Hilaret, N., Gasc, J., Wang, Y., & Green, H. W. (2013). Deep-focus earthquake analogs recorded at high pressure and temperature in the laboratory. *Science*, 341(6152), 1377–1380. <https://doi.org/10.1126/science.1242026>
- Seno, T., Sakurai, T., & Stein, S. (1996). Can the Okhotsk plate be discriminated from the North American plate? *Journal of Geophysical Research*, 101(B5), 11305–11315. <https://doi.org/10.1029/96JB00532>
- Shestakov, N., Ohzono, M., Takahashi, H., Gerasimenko, M., Bykov, V., Gordeev, E., et al. (2014). Modeling of coseismic crustal movements initiated by the May 24, 2013, Mw= 8.3 Okhotsk deep focus earthquake. *Doklady Earth Sciences*, 457(2), 976–981. <https://doi.org/10.1134/S1028334X1408008X>
- Steblov, G. M., Ekström, G., Kogan, M. G., Freymueller, J. T., Titkov, N. N., Vasilenko, N. F., et al. (2014). First geodetic observations of a deep earthquake: The 2013 Sea of Okhotsk Mw 8.3, 611 km-deep, event. *Geophysical Research Letters*, 41(11), 3826–3832. <https://doi.org/10.1002/2014GL060003>
- Ye, L., Lay, T., Kanamori, H., & Koper, K. D. (2013). Energy release of the 2013 Mw 8.3 Sea of Okhotsk earthquake and deep slab stress heterogeneity. *Science*, 341(6152), 1380–1384. <https://doi.org/10.1126/science.1242032>
- Yogodzinski, G., Lees, J., Churikova, T., Dorendorf, F., Wöberner, G., & Volynets, O. (2001). Geochemical evidence for the melting of subducting oceanic lithosphere at plate edges. *Nature*, 409(6819), 500–504. <https://doi.org/10.1038/35054039>
- Zhan, Z., Kanamori, H., Tsai, V. C., Helmburger, D. V., & Wei, S. (2014). Rupture complexity of the 1994 Bolivia and 2013 sea of Okhotsk deep earthquakes. *Earth and Planetary Science Letters*, 385, 89–96. <https://doi.org/10.1016/j.epsl.2013.10.028>
- Zhao, L., Liu, X., Zhao, D., Wang, X., & Qiao, Q. (2021). Mapping the Pacific slab edge and toroidal mantle flow beneath Kamchatka. *Journal of Geophysical Research: Solid Earth*, 126(11), e2021JB022518. <https://doi.org/10.1029/2021JB022518>

## References From the Supporting Information

- Altamimi, Z., Métivier, L., & Collilieux, X. (2012). ITRF2008 plate motion model. *Journal of Geophysical Research*, 117(B7). <https://doi.org/10.1029/2011JB008930>
- Amante, C., & Eakins, B. W. (2009). ETOPO1 arc-minute global relief model: Procedures, data sources and analysis.
- Boehm, J., Werl, B., & Schuh, H. (2006). Troposphere mapping functions for GPS and very long baseline interferometry from European Centre for Medium-Range Weather Forecasts operational analysis data. *Journal of Geophysical Research*, 111(B2), B02406. <https://doi.org/10.1029/2005JB003629>

- Dziewonski, A. M., & Anderson, D. L. (1981). Preliminary reference Earth model. *Physics of the Earth and Planetary Interiors*, 25(4), 297–356. [https://doi.org/10.1016/0031-9201\(81\)90046-7](https://doi.org/10.1016/0031-9201(81)90046-7)
- Herring, T., King, R., Floyd, M., & McClusky, S. (2015). *GAMIT and GLOBK reference manuals: Release 10.6*. Massachusetts Institute of Technology.
- Lyard, F., Lefèvre, F., Letellier, T., & Francis, O. (2006). Modelling the global ocean tides: Modern insights from FES2004. *Ocean Dynamics*, 56(5–6), 394–415. <https://doi.org/10.1007/s10236-006-0086-x>
- Nocquet, J., Villegas-Lanza, J., Chlieh, M., Mothes, P., Rolandone, F., Jarrin, P., et al. (2014). Motion of continental slivers and creeping subduction in the northern andes. *Nature Geoscience*, 7(4), 287–291. <https://doi.org/10.1038/ngeo2099>
- Radiguet, M., Cotton, F., Vergnolle, M., Campillo, M., Valette, B., Kostoglodov, V., & Cotte, N. (2011). Spatial and temporal evolution of a long term slow slip event: The 2006 Guerrero slow slip event. *Geophysical Journal International*, 184(2), 816–828. <https://doi.org/10.1111/j.1365-246X.2010.04866.x>
- Rousset, B., Lasserre, C., Cubas, N., Graham, S., Radiguet, M., DeMets, C., et al. (2016). Lateral variations of interplate coupling along the Mexican subduction interface: Relationships with long-term morphology and fault zone mechanical properties. *Pure and Applied Geophysics*, 173(10–11), 3467–3486. <https://doi.org/10.1007/s00024-015-1215-6>
- Tarantola, A. (2005). Inverse problem theory and methods for model parameter estimation.
- Thomas, A. L. (1993). *Poly 3D: A three-dimensional, polygonal element, displacement discontinuity boundary element computer program with applications to fractures, faults, and cavities in the Earth's crust*. Unpublished master's thesis to the Department of Geology Stanford University.
- Tregoning, P., & van Dam, T. (2005). Effects of atmospheric pressure loading and seven parameter transformations on estimates of geocenter motion and station heights from space geodetic observations. *Journal of Geophysical Research*, 110(B3), B03408. <https://doi.org/10.1029/2004JB003334>